Biochimica et Biophysica Acta 1848 (2015) 1424–1435

Contents lists available at ScienceDirect

Biochimica et Biophysica Acta

journal homepage: www.elsevier.com/locate/bbamem

Docosahexaenoic acid promotes micron scale liquid-ordered domains. A comparison study of docosahexaenoic versus oleic acid containing phosphatidylcholine in raft-like mixtures

R. Georgieva [a], C. Chachaty [b], R. Hazarosova [a], C. Tessier [c,d], P. Nuss [c,d], A. Momchilova [a], G. Staneva [a,*]

[a] Institute of Biophysics and Biomedical Engineering, Bulgarian Academy of Sciences, Acad. G. Bonchev Str., Bl. 21, 1113 Sofia, Bulgaria
[b] Universite Pierre et Marie Curie-Paris 6, INSERM U893, CHU St. Antoine, 27 rue Chaligny, 75012 Paris, France
[c] UMR 7203, INSERM ERL 1057 – Bioactive Molecules Laboratory, Pierre et Marie Curie University, Paris, France
[d] Department of Psychiatry, Hôpital Saint-Antoine, AP-HP, Paris, France

ARTICLE INFO

Article history:
Received 15 October 2014
Received in revised form 24 February 2015
Accepted 26 February 2015
Available online 9 March 2015

Keywords:
Docosahexaenoic acid
Raft
Liquid-ordered phase
Oleic acid
PUFA

ABSTRACT

The understanding of the functional role of the lipid diversity in biological membranes is a major challenge. Lipid models have been developed to address this issue by using lipid mixtures generating liquid-ordered (L_o)/liquid-disordered (L_d) immiscibility. The present study examined mixtures comprising Egg sphingomyelin (SM), cholesterol (chol) and phosphatidylcholine (PC) either containing docosahexaenoic (PDPC) or oleic acid (POPC). The mixtures were examined in terms of their capability to induce phase separation at the micron- and nano-scales. Fluorescence microscopy, electron spin resonance (ESR), X-ray diffraction (XRD) and calorimetry methods were used to analyze the lateral organization of the mixtures. Fluorescence microscopy of giant vesicles could show that the temperature of the micron-scale L_o/L_d miscibility is higher for PDPC than for POPC ternary mixtures. At 37 °C, no micron-scale L_o/L_d phase separation could be identified in the POPC containing mixtures while it was evident for PDPC. In contrast, a phase separation was distinguished for both PC mixtures by ESR and XRD, indicative that PDPC and POPC mixtures differed in micron vs nano domain organization. Compared to POPC, the higher line tension of the L_o domains observed in PDPC mixtures is assumed to result from the higher difference in L_o/L_d order parameter rather than hydrophobic mismatch.

1. Introduction

The understanding of the physiological significance of lipid diversity and dynamic organization in biological membranes is a key issue in membrane research. In particular, the role of the degree of fatty acid (FA) unsaturation such as for omega-3/6 families is an important topic of examination [1–4]. The influence of the FA carbon chain length is also an interesting field of investigation. Phospholipids (PLs) containing saturated FA with cholesterol are known to spontaneously segregate and form clusters such as membrane type "rafts" domains [5–7] which are dynamic and highly ordered domains characterized by their size [8–10] and ability to form sorting platforms for targeted protein traffic and signaling [11,12].

To further understand membrane lipid heterogeneity, biomimetic membrane models have been developed with a various degree of complexity (type, number, and ratio of lipids) using different biophysical methods. For instance, lateral heterogeneity was evidenced by a narrow phase transition for binary mixtures [13] while a liquid ordered/liquid disordered phase separation was described for ternary mixtures comprising high and low melting temperature lipids with cholesterol [14–18]. The liquid ordered (L_o) arrangement characterized by high lateral lipid mobility and dense packing of FA is of biological importance as it is usually considered to model cellular rafts [19]. In particular, the influence of a specific lipid in the formation of L_o domains is still an issue. It was recently shown that sphingolipids, ceramide and sphingosine can promote L_o domain formation [20–25]. With respect to the formation of L_o domains, the role of the FA nature is also to be examined, specifically for docosahexaenoic acid (DHA) containing lipids. Indeed, DHA is believed to influence membrane organization in particular lipid raft formation, and be involved in cell signaling [26,27].

DHA is a polyunsaturated fatty acid (PUFA), belonging to the omega-3 family whose carbon chain is extremely flexible due to a high degree of molecular freedom [28,29]. Data from NMR studies clearly showed the remarkable mobility of DHA chains leading to quite thin and fluid [30], very permeable [31] and elastic [32] membranes.

In the present study, we aimed to examine the role of the degree of unsaturation and FA chain length in the formation and stability of the liquid/liquid phase separation. For this, we compared lipid mixtures only differing in DHA and oleic acid content. Oleic acid (OA), a FA containing one double bond was chosen because it represents the

* Corresponding author. Tel.: +359 2 9793686; fax: +359 2 8723787.
E-mail address: gstaneva@obzor.bio21.bas.bg (G. Staneva).

http://dx.doi.org/10.1016/j.bbamem.2015.02.027
0005-2736/

most common unsaturated FA. Palmitoyl-oleoyl phosphatidylcholine (POPC) is a phospholipid that contains OA at the *sn-2* position, whereas for palmitoyl-docosahexaenoyl phosphatidylcholine (PDPC) the esterified *sn-2* FA is DHA with six conjugated double bonds (Fig. 1). Binary (POPC vs PDPC/EggSM) and ternary (POPC vs PDPC/EggSM/chol) lipid mixtures have been investigated in order to examine and compare their phase separation behavior in a multi-scale approach. Therefore, we have used fluorescence microscopy, electron spin resonance spectroscopy (ESR), X-ray diffraction (XRD) and differential scanning calorimetry (DSC) methods.

2. Material and methods

2.1. Lipids

L-α-phosphatidylcholine-β-palmitoyl-γ-oleoyl (POPC), *L*-α-phosphatidylcholine-β-palmitoyl-γ-docosahexaenoyl (PDPC), sphingomyelin from egg yolk (EggSM) and the fluorescent lipid analog *L*-α-phosphatidylethanolamine-*N*-(lisamine rhodamine *B* sulfonyl) (Rhod-PE) were purchased from Avanti Polar Lipids, Alabaster, and used without further purification. The distribution of fatty acids in egg sphingomyelin is 84% C16:0, 6% C18:0, 2% C20:0, 4% C22:0 and 4% C24:0. The buffer of 0.5 mM Hepes, pH 7.4 (conductance $\sigma = 59$ μS/cm) and doxyl-16-stearic acid spin probe were purchased from Sigma-Aldrich.

All possible precautions were taken during lipid manipulations to minimize oxidation processes [33,34]. Glove box purged with nitrogen was used during all procedures related to vesicle preparations and direct exposure to light was systematically avoided. Buffer used for hydration was depleted of dissolved oxygen by nitrogen gas bubbling.

Only up to 2 week-aged POPC and PDPC solutions were used for our experiment as we could verify using gas chromatography that no significant traces of oxidation was visible up to 2 weeks.

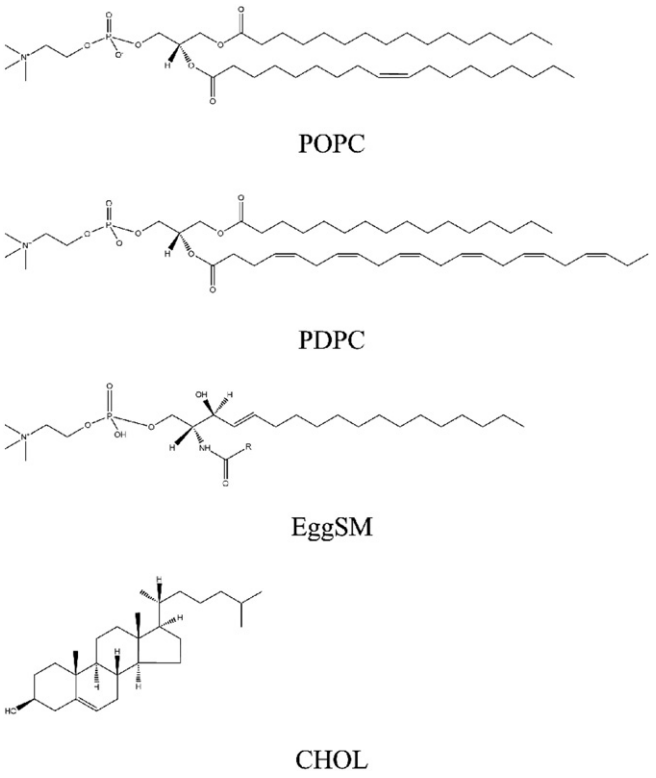

Fig. 1. Molecular structure of the studied lipids from top to bottom as follows: *L*-α-phosphatidylcholine-β-palmitoyl-γ-oleoyl (POPC), *L*-α-phosphatidylcholine-β-palmitoyl-γ-docosahexaenoyl (PDPC), sphingomyelin from egg yolk (EggSM) and cholesterol (chol).

2.2. Methods

2.2.1. Electroformation and fluorescence microscopy of giant unilamellar vesicles (GUVs)

2.2.1.1. Electroformation. Giant unilamellar vesicles (GUVs) were prepared using the electroformation method developed by Angelova and Dimitrov [35]. The lipid mixtures were prepared in diethyl ether/chloroform/methanol (70/20/10 v/v) at 0.5 mg/ml total lipid. Three drops of the lipid solution were spread onto each electrode. The diameters of platinum electrodes were 0.8 mm and they were positioned parallel to each other at a distance of 3 mm. The diethyl ether was used to increase the wetting capacity of the lipid drops on the platinum electrodes. The solvent was evaporated and then the electrodes were placed in a temperature-controlled quartz chamber. The dry lipid layers were hydrated with 0.5 mM Hepes buffer, pH 7.4, $\sigma = 59$ μS/cm. An alternative voltage rising from 100 mV to 400 mV over 30 min with a frequency of 10 Hz was applied. The time for vesicle formation was from 3 to 5 h depending on the type of lipid mixture.

GUVs were observed using a Zeiss Axiovert 135 microscope equipped with 63× long working distance objective lens (LD Achroplan Ph2). Observations were recorded using Zeiss AxioCam HSm CCD camera connected to an image recording and processing system (Axiovision, Zeiss). Lipid phase separation in GUVs was followed in fluorescence by Zeiss filter set 15 (Ex/Em = 546/590 nm).

Protection against oxidation of the GUVs: Several methods were used to avoid oxidation of the studied lipid mixtures. We first used Platinum (Pt) electrodes and low up to 400 mV peak to peak sine wave voltages to minimize the formation of lipid peroxides by electrochemical reactions. To avoid photo-induced oxidation during the fluorescence observation, we used a low power illumination (50 W Hg arc lamp light) along with low dye concentration, neutral density filters up to OD = 1.0 and shorter as possible shutter open time during imaging following recommendations of the Feigenson's group [18,36]. We only accepted as experimental results the phase separation visualized immediately after opening of illumination and not those taken after long exposure time. In order to examine whether lipid oxidation took place and affected L_o/L_d phase separation in GUV membranes, different concentrations of *n*-propyl-gallate (*n*PG) were used from 0.5 to 5 mM. *n*PG was added to the buffer before electroformation of GUV and after it. No differences in phase behavior of the lipid mixtures were noticed with both conditions indicative of the effectiveness of the used protective methods (data not shown). Therefore, we stated that if some lipid oxidation happened during GUV electroformation its influence on lipid phase separation could be considered as negligible under our experimental conditions.

2.2.1.2. Fluorescence microscopy. Fluorescence microscopy method is able to visualize the micron-scale phase separation. The fluorescent lipid marker Egg Rhodamine PE is known to partition predominantly in L_d phase where it appears as bright regions under fluorescence [37]. By contrast, the L_o phase is identified by dark round-shaped domains within the vesicle membrane. Two types of experiments were performed. The first one aimed at determining the temperature of micron-scale miscibility transition. Temperature of domain appearance and disappearance was measured upon cooling and after reheating respectively. The average of these two values could determine the micron-scale miscibility transition temperature (T_m). Visualization and characterization of the phase morphology as a function of temperature were also performed. The vesicles were studied in the temperature range from 65° to 4 °C at rate 0.1 °C/min during both types of experiments.

2.2.2. DSC

Lipid mixtures, co-dissolved in chloroform/methanol 2/1 (v/v), were dried first under nitrogen gas followed by vacuum overnight to ensure the removal of residual organic solvent. Multilamellar vesicles (MLVs)

were prepared by hydrating the lipid mixtures at 3 mg/ml in warm buffer solutions (65 °C): in the first series of experiments 0.5 mM Hepes, pH 7.4 was used while in the second one 0.5 mM Hepes, pH 7.4. MLV solutions were frozen in dry ice and thawed three times in a water bath (65 °C) to ensure the lipid mixing. The samples were vortex-mixed several times for 1 min. DSC measurements were performed using differential scanning microcalorimeter DASM-4 (Biopribor, Pushchino, Russia) with sensitivity $>4.10^{-6}$ cal/K and a noise level $<5.10^{-7}$ W. Samples were loaded into the calorimetric cell at room temperature. Heating and cooling scans were made with a rate of 0.5 °C/min. Three heating and cooling scans were performed for each analysis to ensure thermogram reproducibility. The cooling scan was always presented in the graphs. The thermograms were corrected for the instrumental baseline. The multicomponent thermograms were deconvolved using Origin Software based on nonlinear least-squares minimization. The deconvolution was made on the assumption that the thermograms can be described in terms of a linear combination of more than one independent transition, each approximating a two-state transition [38]. The midpoint transition temperature (T_c), enthalpy change (ΔH) and apparent cooperativity of the transition (the width at half height ($\Delta T_{1/2}$)) were derived from the excess heat capacity curve.

2.2.3. Small and wide angle X-ray diffraction using synchrotron radiation

MLVs for X-ray diffraction studies were prepared by dissolving lipids in chloroform/methanol (2/1, vol/vol) in desired PC/Egg SM/cholesterol molar ratio. The organic solvent was subsequently evaporated under a stream of oxygen-free dry nitrogen at 45 °C and any remaining traces of solvent were removed by a 2-day storage under high vacuum at 20 °C. Dry lipids were hydrated with an equal weight of a 10 mM Tris–HCl, 150 mM NaCl, 0.1 mM $CaCl_2$ (pH 7.5) buffer. The aqueous dispersion of lipids was thoroughly stirred with a thin needle, sealed under argon, and gently shaken at 50 °C during 2 h. The samples were stored under argon at 4 °C. X-ray examination was conducted after 2 h at 65 °C and a 2 h equilibration at 20 °C and after stirring. Acquisition of X-ray diffractograms was made at the I22 the Diamond Synchrotron Radiation station (UK) (www.diamond.ac.uk). Simultaneous small-angle (SAXS) and wide-angle (WAXS) X-ray scattering intensities were recorded (Application SM4691). The duration of the scan was 15 s during which continuous value integration was processed. The camera length (SAXS) was 1.2 m of the sample. Detector calibration was carried out using silver behenate. The lipid dispersion sample (20 μl) was sandwiched between two thin mica windows (0.5 mm apart). The samples were recorded at 37 °C after a 10 min period for temperature equilibration. Data reduction and analysis were performed using Peak Fit 4.12 software (Systat Software Inc.). After X-ray analysis, the fatty acid composition of each phospholipid (POPC, PDPC and EggSM) was examined by gas–liquid chromatography/mass spectrometry to check reproducibility of the samples and confirm that data obtained are based on non-degraded lipids. The small angle X-ray scattering intensity profiles were analyzed using standard procedures [39]. The scattering intensity data from the first four orders of the Bragg reflections of the multilamellar liposomes were used to generate electron density profiles [40] for the L_o and L_d repeat structures detected in the ternary lipid dispersions. After correction of the raw data for detector channel response and subtraction of the background scattering from both water and the sample cell windows, each Bragg peak s was fitted by a Lorentzian + Gaussian distribution. The square root of integrated peak intensity I(h) was derived to determine the form factor F(h): $F(h) = h\sqrt{I(h)}$, h = order of peak reflection, I(h) = integrated intensity of each respective reflection. Electron density profiles were calculated by the Fourier synthesis: $\rho(z) = \sum \pm F(h)\cos(2\pi h\ z/d)$, d = d spacing = dpp + dw (dpp: phosphate–phosphate bilayer thickness, dw: hydration layer). These curves are sigmoidal functions where the maxima are indicative of the electron-enriched membrane region and stand for the phosphorus polar head-group, while the minima represent the electron-deprived area, standing for the fatty acid tail at the center of the bilayer.

2.2.4. ESR methods

X-band ESR experiments have been carried out to extend the range of our observations to the nanometer scale and to determine the effect of DHA on the molecular ordering of the coexisting phases (L_β (gel phase)/L_d (liquid-disordered phase) or L_o (liquid-ordered phase)/L_d). For that purpose we used a doxylstearic acid spin probe labeled in position 16 of the chain (denoted hereafter 16NS) over the temperature range from 17 °C to 57 °C by 5° step. Lipid mixtures were doped with 0.1 mol% of 16NS. After evaporation of the solvent the dry lipids were hydrated with a large excess 500 μl of buffer consisting of 10 mM Tris–HCl, pH 7.5, 150 mM NaCl, and 0.1 mM $CaCl_2$. The lipid dispersion was centrifuged and 20 μl of the pelleted liposomes were transferred to an ESR measurement capillary cell and sealed.

Continuous wave ESR spectra were recorded at 9.5 GHz (ELEXSYS 500 spectrometer Bruker, Wissembourg, France) after an equilibration time (ca. 10 min) at each temperature set by the variable temperature device. The experiments were systematically ran at microwave powers of 1 and 10 mW, the latter being used to optimize the S/N ratio. No saturation effects were observed. Moreover the reversibility with temperature of the recordings was checked.

The ESR parameters have been determined by least-squares spectral fittings as previously reported [41] (see also www.esr-spectsim-softw.fr).

The quality of fittings was evaluated from the average standard deviation $\boldsymbol{\sigma}$ between the normalized experimental and computed spectra. For each samples $\boldsymbol{\sigma}$ was generally found in the order of 0.07 and 0.05 for microwave powers of 1 and 10 mW, respectively. As the difference is very small, we have considered the mean values of the parameters derived from these two series of measurements.

These fittings are generally inconsistent with a single site. It is therefore assumed that the spin probe is distributed among two or tentatively among three sites each one corresponding to a L_d, L_β and/or L_o phases. The adjustable parameters of major interest are the order parameter $S_{zz} = (a_{//} - a_\perp)/(a_{zz} - \frac{1}{2}(a_{xx} + a_{yy}))$ in the most ordered L_β, L_o (A) and less ordered L_d (B) phases and the effective reorientation correlation time τ in each of these phases as well as the fraction of the probe in the most ordered one (L_β or L_o phase). a// and a⊥ are the principal values of the nitrogen hyperfine coupling tensor **a** averaged by the motions about the directory of the lamellar phases. Here we have taken for the **a** tensor a_{zz} = 3.29mT, a_{yy} = 0.54mT, a_{xx} = 0.59mT and g_{zz} = 2.0022, g_{yy} = 2.0058, g_{xx} = 2.0088 for the **g** tensor [42], the Z and X axes being directed along the axis of the nitrogen centred $2p_z$ orbital and the N – O bond, respectively. As the **a** tensor is dependent on the local polarity, its principal values have been corrected by a factor taken as an adjustable parameter of spectral fittings. τ is an effective reorientation correlation time resulting from the wobbling of the probe about the director of the phase, from its overall axial reorientation and from segmental motions. In most cases however it follows approximately the $\tau = \tau_0 \exp(E/RT)$ temperature dependence. Its mean value $\langle\tau\rangle_{T\ min}^{T\ max}$ over a temperature range may be useful to compare the molecular mobility at the level of the probe in different mixtures.

The reliability in the determination of the most ordered fraction and Szz A and Szz B displayed in Figs. 6 and 7 can be estimated from the differences in the fittings of spectra recorded at powers 1 mW and 10 mW. Denoting F one of these parameters, the reduced difference between each of the two series of measurement is expressed as:

$$R = |F(10mW) - F(1mW)|/0.5 \times [F(10mW) + F(1mW)]$$

The mean values of R over all binary and ternary mixtures are 0.06, 0.04 and 0.008 for fraction A, Szz A and Szz B, respectively.

3. Results

All studied methods aimed at comparing phase behavior differences between DHA- and OA-containing PCs.

3.1. Fluorescence microscopy study

Fluorescence microscopy method allowed measurement of the temperature values of micron-scale L_o/L_d phase miscibility. The results for POPC/EggSM/chol and PDPC/EggSM/chol ternary mixtures are shown in Table 1.

3.1.1. PCs/EggSM/chol (50/25/25 mol/mol/mol) mixtures

A phase separation of ternary lipid mixtures 50/25/25 POPC/EggSM/chol and PDPC/EggSM/chol is demonstrated in the temperature range from 40° to 4 °C (Fig. 2).

In the POPC-ternary mixture, homogenous vesicles were observed from 40° to 24 ° C (Fig. 2a). At 23.4 °C, small dark domains characterized by a perfectly round shape appeared on a bright background, demonstrating the coexistence of two liquid phases (Table 1). With temperature decrease they began to grow by fusion (Fig. 2b). A phase percolation was observed at temperatures between 13 and 4 °C (Fig. 2c) with many bright domains in L_d phase moving on a dark background.

In the PDPC-mixture, a phase separation was detected within a wider temperature range starting from 49.8° to 4 °C (Table 1, Fig. 2(d–f)). The miscibility temperature of this mixture is 26.4 °C higher than that of the POPC one. At the lowest temperatures, the L_o domain fraction predominates within the Ld phase (Fig. 2f) in contrast with the POPC mixture where the converse is observed with L_d domains prevailing into a L_o phase (Fig. 2c).

3.1.2. PCs/EggSM/Chol (40/40/20 and 34/33/33 mol/mol/mol) mixtures

A greater molar percentage of SM and chol into the mixtures increased the temperature of micron-scale miscibility transition in both types of PC-containing mixtures (Table 1).

In the PDPC-mixtures, L_o/L_d phase separation occurred at much higher temperatures (62.4 °C for 40/40/20 and 60.2 °C for 34/33/33) compared to the POPC ones (32.5 °C and 30.3 °C respectively). It can be concluded that the presence of DHA instead of OA in PC increases significantly the temperature of L_o/L_d miscibility of the mixture. The L_o domain size was larger for PDPC containing mixtures compared to POPC ones at physiological temperature.

3.2. DSC study

DSC could evidence in single EggSM a highly cooperative gel to fluid phase transition with a high melting temperature (T_m = 39.7 °C) with 7.9 kcal/mol enthalpy (Fig. 3A, Table 2). In contrast, POPC and PDPC exhibited similar thermal behavior with phase transition temperature at about −3 °C [43].

The addition of 10 mol% chol to EggSM led to a binary mixture exhibiting a larger transition peak and a significant enthalpy reduction (1.3 kcal/mol) (Fig. 3B). The observed asymmetrical transition peak was deconvolved into two components, allowing calculation of transition temperatures, enthalpies and apparent cooperativity values for each of the two components (Table 2). This result is in accordance with studies showing that peak asymmetry is observed in binary mixtures of natural sterols with saturated PCs [44,45]. The first peak, denoted as phase I, was centered at 37.9 °C, while the second (phase II) was measured at 41.1 °C (Fig. 3B, Table 2). Previous studies have assigned these two phases to cholesterol-poor and cholesterol-enriched phases respectively [46,47]. In these studies, it has been demonstrated that the transition temperature and cooperativity of phase I decreased slightly with the increase of cholesterol concentration while the enthalpy decreased significantly. This component disappeared completely at high cholesterol concentrations (50 mol%).

The phase transition temperature of the second component (phase II), however, increased with augmentation of the cholesterol content, while the cooperativity decreased significantly. The enthalpy of phase II initially increased, was followed by a reduction reaching zero at a concentration of 50 mol% chol [46,47]. In our study, the addition of POPC and PDPC (85/10/5 EggSM/chol/PCs mixtures) shifted the transition to lower temperatures, increased enthalpy and broadened largely the transition compared to the described binary mixture (90/10 EggSM/chol) (Fig. 3C, Table 2). Phase transition temperature of components I and II decreased for both PC mixtures. At a temperature of about 45 °C, a significant fraction of lipids could not melt in the PDPC containing mixture whereas this was not observed for the POPC ternary mixture (Fig. 3C). The 5% PDPC addition was associated with a significant enthalpy increase for both phases I and II while the same amount addition of POPC led to little changes in phase II (Table 2). Accordingly, in the PDPC mixture a higher T_m, enthalpy phase was observed with a lower apparent cooperativity compared to POPC. The effect of POPC seemed to be more pronounced on phase I than phase II compared to the EggSM/chol control mixture. POPC tended to interact with phase I (cholesterol-poor phase) unlike the PDPC mixture. PDPC affected both components indicating that it substantially affected the lipid distribution in two phases.

Mannock et al. [48] could evidence in EggSM/chol mixture that cholesterol increment led to an increased phase transition temperature along with a marked decreased cooperativity. These thermotropic properties were rather attributed to the broad component (with higher melting temperature) than the sharp one (with lower melting temperature). These results support the assumption that addition of DHA containing PC can induce a decreased miscibility of cholesterol in phase I consequently leading to more cholesterol in phase II. Thus, the higher melting temperature and enthalpy of phase II in the PDPC mixture are assumed to result from an increased cholesterol concentration in the EggSM/chol mixtures [48].

In conclusion, the addition of 5% DHA in the EggSM/chol mixture was able to form a phase with higher melting temperature and enthalpy compared to the same amount addition of POPC, suggesting that cholesterol distribution between the co-existing phases of the studied mixture is not the same for both PCs.

Table 1
L_o/L_d micron-scale miscibility transition temperatures (T_m) of POPC/EggSM/chol and PDPC/EggSM/chol ternary mixtures studied by fluorescence microscopy.

Sample and molar ratio	$T_{Lo/Ld\ micron\text{-}scale\ miscibility}$ (°C)
POPC/EggSM/chol	
40/40/20	32.5 ± 3.5
34/33/33	30.3 ± 2.6
50/25/25	23.4 ± 2.4
PDPC/EggSM/chol	
40/40/20	62.4 ± 2.3
34/33/33	60.2 ± 1.9
50/25/25	49.8 ± 2.0

3.3. Small angle X-ray study

PDPC and POPC ternary mixtures lipid organization was studied and compared using X-ray scattering method in order to identify phase separation behavior by d-spacing and bilayer thickness (dpp) measures. Both PC-enriched mixtures (PCs/EggSM/chol 50/25/25 mol/mol/mol) were compared at temperatures of 20 °C, 30 °C, and 37 °C (Table 3). SAXS diffractograms (raw data) can be viewed in the supplementary data section (Fig. A).

The splitting of the diffraction peaks revealed the heterogeneity for both studied mixture (Fig. 4). At all studied temperatures, a lamellar liquid–liquid phase separation was observed for POPC and PDPC (except at 20 °C for the POPC mixture where no phase separation was detected).

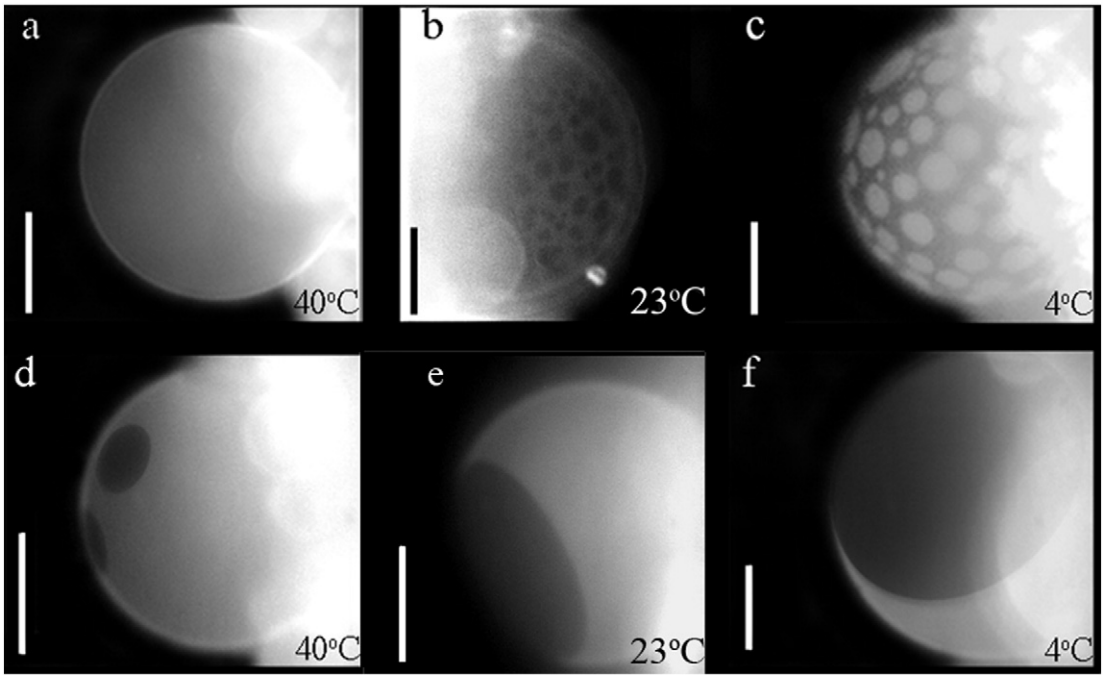

Fig. 2. Effect of the degree of fatty acid unsaturation/chain length in DHA and OA containing PC on the formation of L_o/L_d phase separation. A fluorescent lipid marker, egg Rhodamine PE was used to visualize the formation of micron-scale domains. Vesicles composed of POPC/EggSM/chol (a–c) and PDPC/EggSM/chol (d–f) (50/25/25 mol/mol/mol) mixtures are shown in the temperature range from 40° to 4 °C. POPC vesicles are uniform in the temperature range 40 °C–24 °C (a). Domains in L_o phase appear at 23.4 °C (images are shown at lower temperature (23 °C) for their better visibility of the domains (b)). Phase percolation (continuous L_o with bright domains in L_d phase) is seen from 13° to 4 °C (c). In PDPC-vesicles, L_o/L_d phase separation occurs in the wide temperature range from 50° to 4 °C (d–f). L_o domains are formed at 49.8 °C. At 4 °C, the fraction of L_o domains takes from one half to two thirds of the vesicle surface (f). Scale bars: 20 μm.

Among mixtures exhibiting phase separation, two lamellar liquid phases (L1 phase/L2 phase) were identified at all studied temperatures for each of the four identified Bragg peak order, except at 30 °C for the PDPC mixture where a third lamellar phase was distinguishable. The L1 (long d-spacing component) and L2 (short d-spacing component) phases have been assigned to L_o and L_d phases respectively. Analysis of the bilayer thickness (dpp) indicated greater dpp values for PDPC in comparison to POPC for L_o and L_d phases at all studied temperatures (Table 3). Thermal behavior of dpp is specific for each L_o and L_d phases for both PCs mixtures. For L_o phase, no change in dpp value was observed with temperature increase in the POPC mixture while temperature increase was associated with dpp decrease for PDPC. For L_d phase, the POPC mixture exhibited a dpp decrease with temperature elevation, whereas the opposite was observed for PDPC with a dpp augmentation with temperature increase. It can be concluded that the phase separation observed in both mixtures does not result only from dpp difference between the coexisting phases that are resulting from the hydrophobic mismatch between two phases. Indeed, in the studied PDPC mixture a phase separation was still maintained at 37 °C despite no major difference in dpp between L_o/L_d phases.

Other molar ratio ternary mixtures (40/30/30 and 34/33/33) were also studied (data not shown). The reason why these data are not shown is that SAXS peaks were rather symmetrical under our experimental conditions. However, the absence of multiple peaks does not imply the absence of phase separation, because the coexisting phases with similar D- or d-spacings may not be resolved. The small difference in FA length between two PCs species is probably additionally diminished by cholesterol that may impede the resolving of phase coexistence. Only the most PC-enriched mixtures have been described in this section because splitted or asymmetrical SAXS peaks have been found up to 4th order.

3.4. ESR study

The motion and order in binary PCs/EggSM and ternary PCs/EggSM/chol mixtures were investigated by ESR spectroscopy of a spin-labeled fatty acid with the nitroxide reporter group attached at position 16 of the acyl chain (16NS) to probe the environment of the bilayer center. Order parameters and reorientation correlation times were derived from a spectral simulation analysis.

3.4.1. Binary mixtures

The two component spectra are assigned to the coexistence of the gel (L_{β}) and L_d phases in the studied temperature range. The L_{β} phase disappeared at the vicinity 42° and 32 °C for the POPC/EggSM and PDPC/EggSM 50/50 mixtures, respectively. Both the order parameter Szz and fraction of L_{β} were larger for POPC than PDPC in the whole temperature range. For the L_d phase, Szz was nearly equivalent for both mixtures (Fig. 5). It may be pointed out that in the temperature range of coexistence of L_{β} and L_d phases, the mean reorientation correlation times $\langle\tau\rangle_{17^\circ}^{32^\circ}$ in the L_{β} and L_d phases were quite close: 0.68 and 0.64 ns, 0.60 and 0.59 ns for the POPC/EggSM and PDPC/EggSM mixtures, respectively (Table 4).

3.4.2. Ternary mixtures

The influence of the sample composition on Szz and on the fraction of the probe among the phases has been investigated on PCs/EggSM/chol 50/25/25, 40/40/20 and 34/33/33. By analogy with the fluorescence microscopy study, PC denotes POPC or PDPC. The visual inspection of ESR spectra revealed the existence of at least two sites differing by the relevant Szz values (Fig. 6). The spectral simulations were indeed consistent with the coexistence of two phases characterized by $0.25 < Szz < 0.4$ and $0.05 < Szz < 0.2$ assigned to the L_o and L_d phases, respectively.

As apparent in Table 4 in the case of the POPC/EggSM/chol mixtures $\langle\tau\rangle_{17^\circ}^{52^\circ}$ is significantly smaller for the L_o than for the L_d phase indicating a higher molecular mobility in the former. The same is true but to a lesser extent for the PDPC/EggSM/chol mixtures. To explain this difference we have tentatively assumed the coexistence of three phases L_{β}, L_o and L_d or L_o, L_{d1} and L_{d2}. In most cases the spectral simulations yield inconsistent or spurious values of parameters so that this assumption probably does not hold. A common feature to the three mixtures is that the order

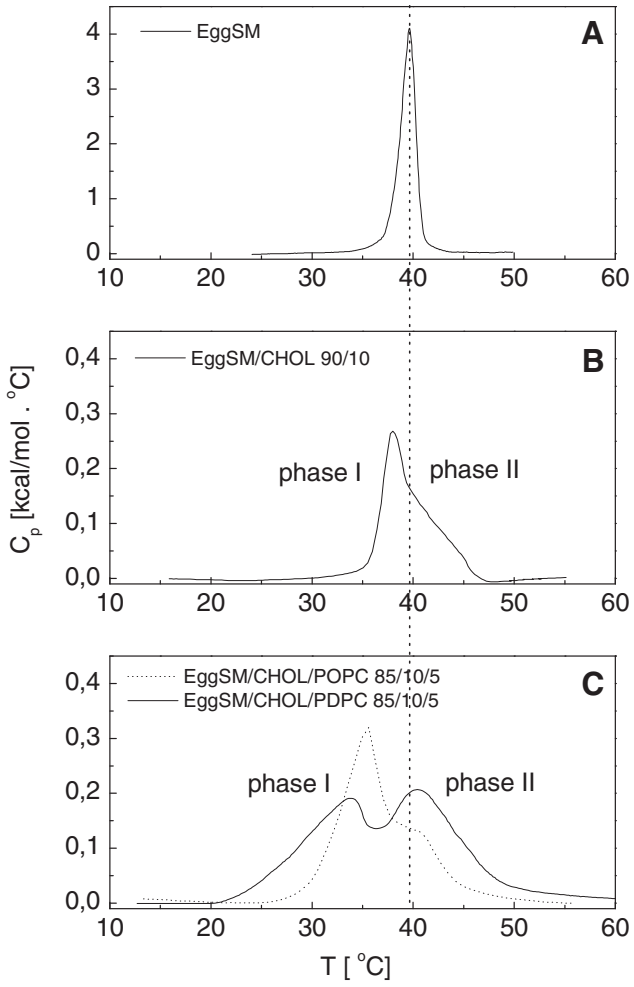

Fig. 3. Representative DSC scans of multi-lamellar vesicles generated from EggSM (A) and 90/10 EggSM/chol binary mixture (B). Comparative analysis of POPC and PDPC in 85/10/5 EggSM/chol/POPC and EggSM/chol/PDPC ternary mixtures (C).

parameter and the mean reorientation correlation times $\langle\tau\rangle_{17^\circ}^{32^\circ}$ of the L_o phase were larger for the PDPC/EggSM/chol mixtures than for the POPC/EggSM/chol ones (Fig. 7a). The reverse is observed for the L_d phase showing that cholesterol is partitioned among the two phases, L_o and L_d being enriched and depleted in this component, respectively. Increasing the POPC and PDPC concentration with respect to EggSM resulted in lowering of the order parameter in the L_o phase (Fig. 7a). The difference in orders between L_o and L_d phases was larger in the PDPC ternary mixtures compared to the POPC. Comparing the 40/40/20 POPC/EggSM/chol and PDPC/EggSM/chol mixtures showed that the difference in Szz

Table 2
Thermodynamic parameters of the gel-fluid phase transitions shown in Fig. 3, average values ± SD (n = 3).

Sample (molar ratio)	Midpoint transition temperature [°C]	ΔH [kcal/mol]	$\Delta T_{1/2}$ [°C]
EggSM	39.7 ± 0.18	7.9 ± 0.11	1.7 ± 0.03
EggSM/chol (90/10)	37.9 ± 0.22	1.3 ± 0.12	4.1 ± 0.06
Phase I	37.9 ± 0.22	0.7 ± 0.12	2.5 ± 0.05
Phase II	41.1 ± 0.31	0.6 ± 0.14	3.7 ± 0.14
EggSM/chol/POPC (85/10/5)	35.6 ± 0. 83	2.5 ± 0.23	5.7 ± 0.09
Phase I	34.9 ± 0.76	1.9 ± 0.23	4.4 ± 0.12
Phase II	40.6 ± 0.89	0.5 ± 0.27	4.3 ± 0.18
EggSM/chol/PDPC (85/10/5)	40.4 ± 0. 91	3.5 ± 0.38	16.5 ± 0.21
Phase I	32.9 ± 0.89	1.6 ± 0.37	7.7 ± 0.23
Phase II	40.7 ± 0.93	1.9 ± 0.41	7.7 ± 0.26

Table 3
Small angle X-ray scattering parameters calculated after deconvolution of diffractograms from POPC and PDPC ternary mixtures (50/25/25 mol/mol/mol) at 20 °C, 30 °C, and 37 °C. Bilayer thicknesses (dpp), lamellar d-spacing, and number of lamellar phases are indicated. All plotted and calculated values are estimated with a ±0.03 nm accuracy.

Sample and studied temperatures	L1 phase		L2 phase		L3 phase		Number of phase
	dpp (nm)	d-spacing (nm)	dpp (nm)	d-spacing (nm)	dpp (nm)	d-spacing (nm)	
POPC/EggSM/chol 50/25/25							
37 °C	4.49	6.70	4.30	6.30			2
30 °C	4.49	6.50	4.41	6.32			2
20 °C	4.49	6.49					1
PDPC/EggSM/chol 50/25/25							
37 °C	4.61	6.81	4.59	6.49			2
30 °C	4.59	6.49	4.50	6.30	4.40	6.00	3
20 °C	4.71	6.60	4.49	6.49			2

of the L_o phases becomes larger when SM/chol ratio reaches 2/1. Additionally, when total cholesterol concentration was elevated in the mixture, the Szz of the L_o phase increased as well suggesting the formation of more stable complexes between cholesterol and SM [49]. In the lowest temperature range, the L_o fraction of POPC/EggSM/chol was larger than for the PDPC/EggSM/chol (Fig. 7b). The reverse was observed above 37 °C where the L_o fractions of PDPC-comprising mixtures were slightly higher. In conclusion, the L_o phase in the presence of PDPC is characterized with higher order and reorientation correlation times than POPC ternary mixtures. These physicochemical properties of the L_o phase in PDPC mixtures probably determine its slightly higher thermo-stability above the physiological temperature compared to the POPC-mixture.

4. Discussion

The present study examined the phase separation behavior of binary and ternary DHA versus OA-comprising PC mixtures. Overall differences in phase separation could be demonstrated between POPC and PDPC mixtures depending on the examination method used, type and number of the associated lipids. A particular emphasis was made on comparing micron and nano-scale lipid organization. With respect to phase separation, we could demonstrate with fluorescence methods that the thermal behavior of both PC species differed in PC/SM/chol mixtures. The L_o/L_d miscibility temperature was higher with larger L_o domain size for PDPC mixtures compared to POPC ones. Interestingly, while fluorescence assays could evidence a phase separation at 37 °C only for the PDPC mixtures, in contrast X-ray diffraction could demonstrate the existence of a L_o/L_d lamellar phase separation for both PC mixtures. ESR was also able to identify two phases for both PC mixtures distinguishable via their order parameters and fraction.

4.1. DHA vs OA containing PC mixtures in membrane models

The effect of the phospholipid head group structure along with acyl chain length and degree of unsaturation upon the tendency to form ordered domains with cholesterol is an interesting and relevant topic of investigation. Among PUFAs, DHA was shown to be preferentially esterified to PE with lesser amounts to PC [50–52]. The distribution within the membrane layer of PE and PC also differs with PE predominating internally while PC being more abundant in the external leaflet [53] and involved in raft formation. A much greater tendency to accumulate with cholesterol and SM in domains mimicking the lipid composition of rafts is implied for PDPC over PDPE, partly because of the smaller head group of PE compared to SM [54]. The present study aimed to investigate both directions: the role of the head group nature that was compared with similar PE experiments in the literature as well as examining the micro vs nano-scale behavior of POPC and PDPC in SM/chol mixtures.

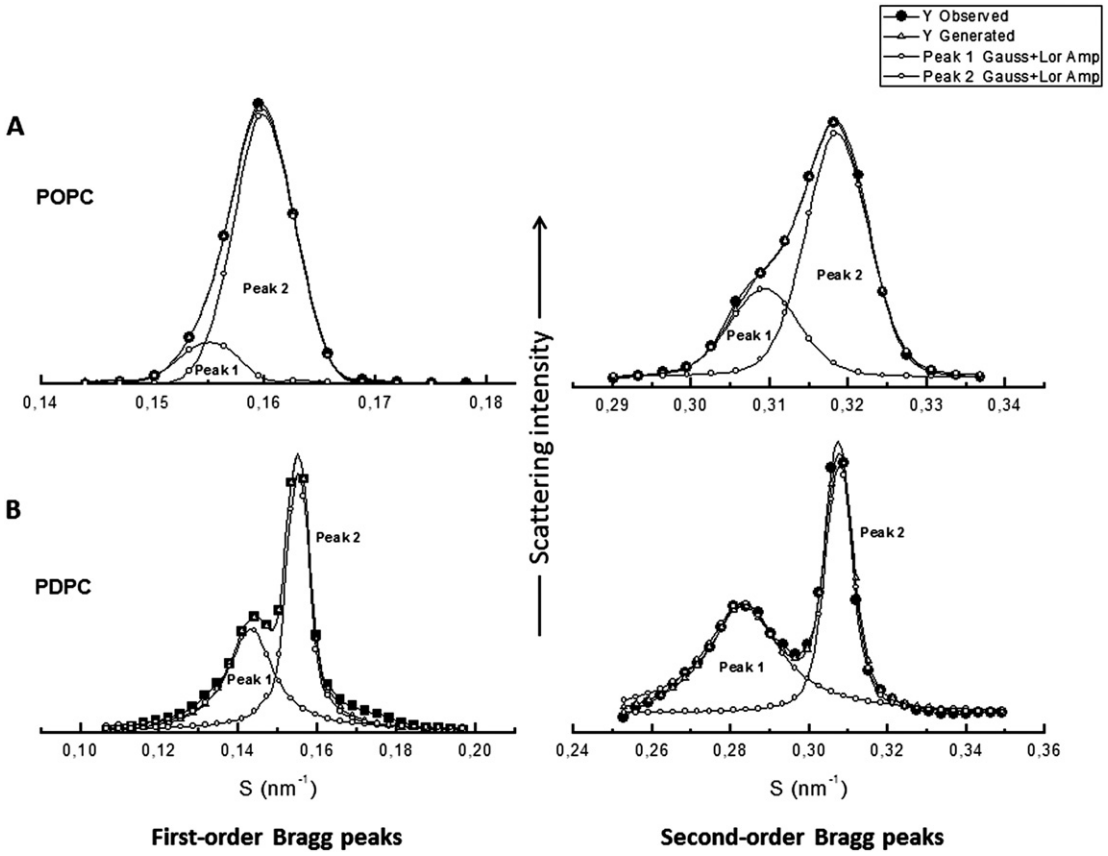

Fig. 4. Peak fit analysis (Gaussian/Lorentzian) of the first two orders of the Bragg scattering intensity peaks (filled circles for Y observed) in the small-angle region at 37 °C for (A) 50/25/25 POPC/EggSM/chol and (B) 50/25/25 PDPC/EggSM/chol. Two coexisting lamellar phases (open circles) are identified by deconvolution and assigned to L1 (peak 1, long d-spacing) standing for liquid-ordered component and L2 (peak 2, short d-spacing) standing for liquid-disordered component.

4.2. DHA-containing PCs are found in L_o domains where they increase the order parameter

DHA and OA containing PC species exhibited differences in phase separation into raft-like domains in model membranes. These differences have been attributed to the saturated nature of sphingolipid acyl chains that packs well with the rigid cholesterol backbone and separate from DHA containing phospholipids. DHA chains are disordered and enhance the segregation of cholesterol into SM-rich/sterol-rich rafts, favoring DHA-rich domains via cholesterol exclusion but DHA chains can also partition into rafts [55].

Our data are in favor of an enriched model also supported by studies such as these developed in mouse B-cell lipid rafts [56] in which PUFA-containing phospholipids can occupy and modify the ordered packing

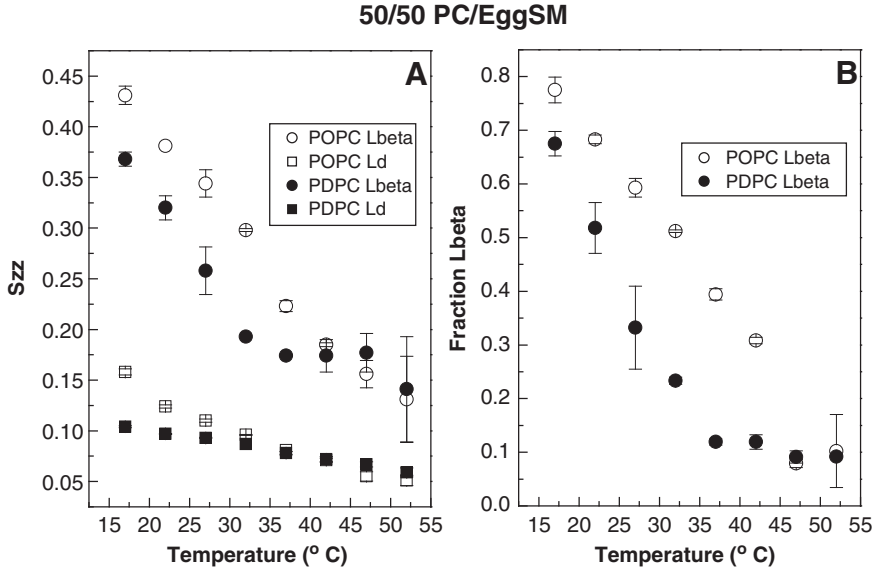

Fig. 5. Order parameters (A) and L_β fractions (B) in 50/50 POPCs/EggSM and PDPC/EggSM binary mixtures.

Table 4
Parameters of spin-label motion in binary PCs (POPC or PDPC)/EggSM and ternary mixtures of PCs (POPC or PDPC)/EggSM/chol; Reorientation correlation times and activation energies.

Mixture (molar ratio)	Sites	τ 32° (ns)	E (kJ/mol)	$\langle\tau\rangle_{17}^{32^\circ}$ (ns)
50/50				
POPC/EggSM	L_β	0.46	36.5	0.68
	L_d	0.55	14.4	0.64
PDPC/EggSM	L_β	0.31	60.2	0.6
	L_d	0.44	28.3	0.59
		τ 37° (ns)		$\langle\tau\rangle_{17}^{52^\circ}$ (ns)
50/25/25				
POPC/EggSM/chol	L_o	0.07	65.3	0.12
	L_d	0.65	16.8	0.71
PDPC/EggSM/chol	L_o	0.29	19.6	0.32
	L_d	0.4	9.5	0.42
40/40/20				
POPC/EggSM/chol	L_o	0.09	71.3	0.17
	L_d	0.61	16.4	0.66
PDPC/EggSM/chol	L_o	0.34	21.3	0.38
	L_d	0.42	9.95	0.44
34/33/33				
POPC/EggSM/chol	L_o	0.13	38.1	0.17
	L_d	0.72	14.3	0.77
PDPC/EggSM/chol	L_o	0.24	18.3	0.26
	L_d	0.53	7.5	0.55

existing within lipid rafts. PUFA can thus be considered both as infiltrating rafts as well as forming (non-raft) domains. Examples of this assumption are numerous. For instance, it could be demonstrated that the DRM fractions derived from neonatal cardiomyocytes contain about 15% OA and 7% DHA at 4 °C [57]. Using model membranes, the same group could measure the amount of POPE or PDPE present in DRM in POPE or PDPE/SM/chol mixtures (POPE: 1-palmitoyl-2-oleoyl-sn-glycerophosphatidylethanolamine; PDPE: 1-palmitoyl-2-docosahexaenoyl-sn-glycerophosphatidylethanolamine). They find twice as much OA than DHA in the DRM fractions (60% vs 20% at 40 °C and 80% vs 30% at 4 °C). DHA-containing PE versus PC mixtures exhibits significant differences in that respect. While a minimal incorporation of PDPE was observed into raft-like domains with PDPE preferentially segregating into non-raft domains, it was demonstrated that a substantial amount of DHA-containing PC can penetrate raft-like domains [54]. The nature of the contained PUFA is also of importance as in studies comparing EPA versus DHA containing PE, incorporation into rafts was twofold greater for DHA than for EPA, indicating that

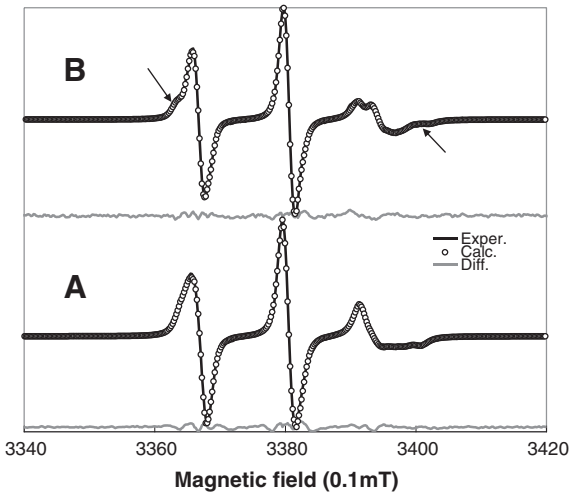

Fig. 6. Experimental and computed ESR spectra of 16NS in 34/33/33 POPC/EggSM/chol (A) and PDPC/EggSM/chol (B). In B the arrows indicate two partially resolved bands providing direct evidence of two sites.

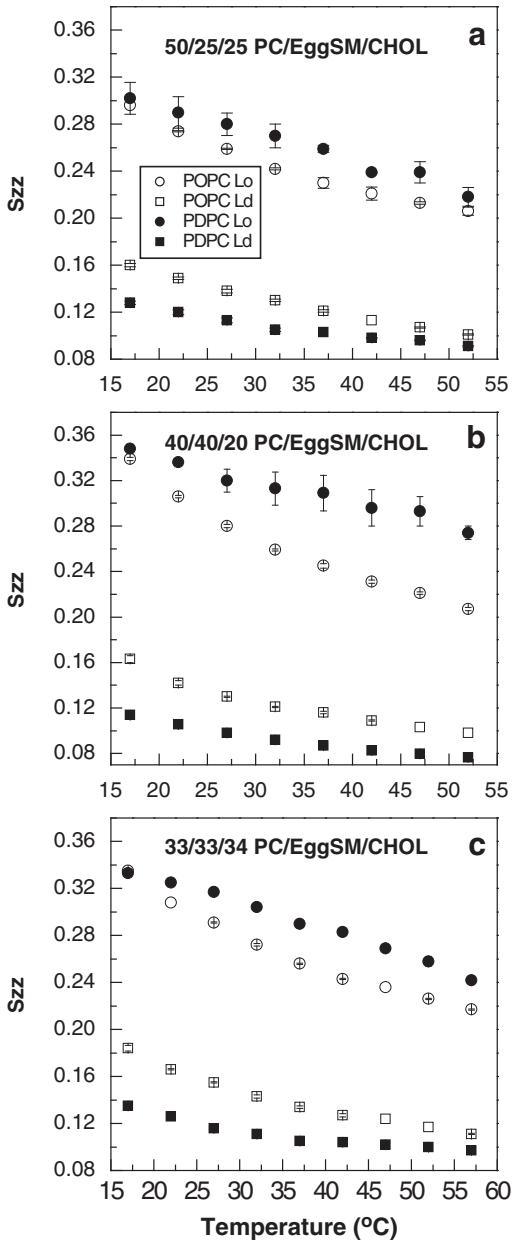

Fig. 7a. Order parameters of the 16 NS spin-labeled probe as a function of the temperature in POPC/EggSM/chol and PDPC/EggSM/chol mixtures (50/25/25 (A), 40/20/20 (B), 34/33/33 (C)).

the longer acyl chains were favoring intrusion into the dense SM/chol packing of the L_o phase [58]. In addition, a recent study in animal with DHA-enriched diet and cultured cells was able to demonstrate that DHA enhances raft formation in plasma cell membranes [59].

4.3. L_o/L_d phase separation in PC mixtures: respective contribution of micro- and nano-scale methods

The differences in phase segregation behavior in both PC mixtures have been examined in comparing our data for each method and matching them with those from the literature. In fluorescence, the temperature of L_o/L_d miscibility was twice as great for the PDPC mixtures as for the POPC ones. This result is in agreement with Garcia-Saez et al. findings using doubly unsaturated PC in their experiments [20,60]. A proportional relationship between the temperature of L_o/L_d phase separation and hydrophobic mismatch was demonstrated. In their experiments, the hydrophobic mismatch was studied as a function of

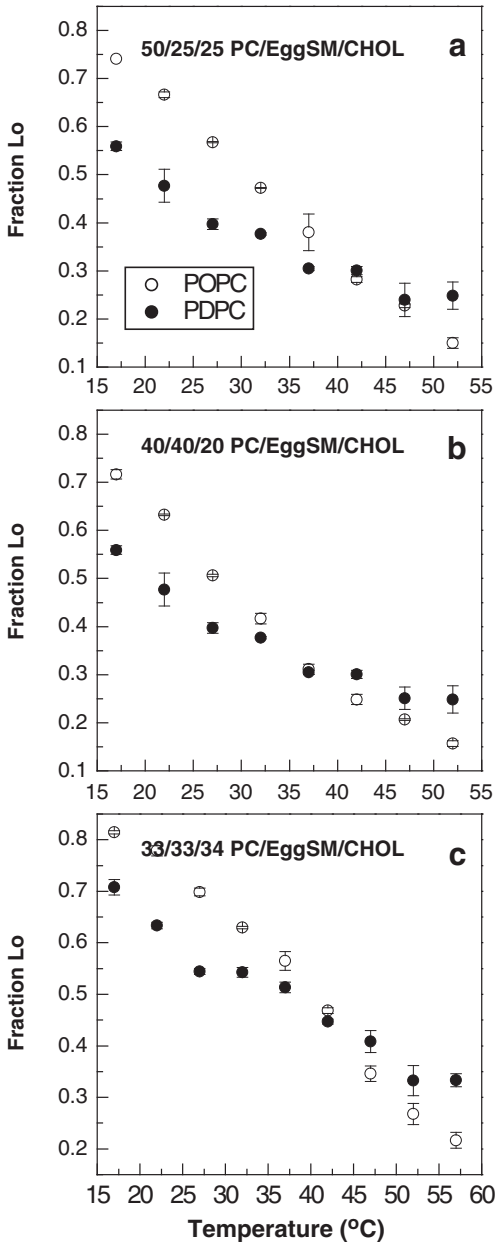

Fig. 7b. L_o fractions of the 16 NS spin-labeled probe as a function of the temperature in POPC/EggSM/chol and PDPC/EggSM/chol mixtures (50/25/25 (A), 40/20/20 (B), 34/33/33 (C)).

the acyl-chain length and degree of unsaturation. The authors could find that the greater the L_o/L_d height mismatch, the higher the de-mixing temperature. In the present study, the larger L_o domain size identified at 37 °C for the PDPC mixtures is in accordance with the higher de-mixing temperature of this mixture compared to the POPC one. The authors have also shown that a twofold change in de-mixing temperature was associated with a two- to fourfold higher line tension of L_o domains. Accordingly, it may be proposed, that the line tension of the L_o domains in our studied PDPC mixtures is higher compared to the POPC ones.

The observed difference in the L_d bilayer thickness for both PC mixtures (Table 3) is in accordance with their fatty acid length. Interestingly, at 37 °C the bilayer thicknesses of L_o and L_d are identical for the PDPC mixture while a L_o/L_d thickness difference is observed for the POPC mixture. It can be concluded that the observed lamellar phase separation in both PC mixtures does not originate from the L_o/L_d bilayer thickness difference only. In the POPC mixture, the L_o/L_d bilayer thickness difference did not translate into a micron-scale L_o/L_d phase separation in GUVs suggesting that the hydrophobic mismatch is not the only parameter that governs the phase separation. In contrast, the negligible bilayer thickness difference between L_o and L_d in PDPC mixtures was not an obstacle in the formation of a phase separation at the nano-and micron-scale, assuming the existence of another driving force causing phase separation in particular related to the mode of acyl chain packing.

4.4. Acyl-chain packing in L_o/L_d phases in POPC/PDPC mixtures

The ESR data contributed to the understanding of the acyl chain packing into the PC mixtures via measures of the order parameter. The L_o order parameter was systematically higher for PDPC compared to POPC, indicative of a greater amount of SM and/or cholesterol in the L_o phase for the PDPC mixtures. A greater order for PDPC in L_o phase was also found using ^{2}H NMR spectroscopy study showing a twofold greater increase in molecular order after cholesterol addition in PDPC/SM- versus PDPE/SM-mixture (1/1/1) at 40 °C [58,61]. Such finding was also demonstrated in animals with fish oil enriched diet [61].

The larger delta Szz difference between L_o and L_d was found for PDPC compared to POPC mixtures. This difference suggests that both PC mixtures exhibit a specific fluidity, spontaneous curvature for each of the two co-existing phases generating differences in line tension along the domain boundaries [62]. The line tension governs the distribution of domain sizes, which may explain the observed differences in behavior between POPC and PDPC mixtures in domain sizes. Higher delta Szz L_o/L_d is an indication that higher line tension can account for the higher temperature of de-mixing in the PDPC mixtures compared to POPC ones rather than the L_o/L_d hydrophobic mismatch. Lower delta Szz L_o/L_d for POPC compared to PDPC mixtures implies a lower line tension for the domains in POPC mixtures leading to smaller domain size for POPC explaining why they are only visible when using nanoscale methods.

Theoretical works predict that the small value of line tension is a factor which would distribute the raft area over smaller raft sizes because of the competition between reduced boundary energies and unfavorable entropy with raft merger [62]. Generally, the average domain size $\overline{R} = 2\sqrt{D_L \times \nu_{ex}^{-1}}$ could be estimated by the ESR method from the exchange rate ν_{ex} of the probe between the L_o and L_d domains and its lateral diffusion coefficient D_L likely of the order of 10^{-11} m^2s^{-1} [63]. For all the mixtures under study, the exchange rate of the probe is below the threshold of ESR measurements $\nu_{ex} \approx 10^6$ s^{-1}. No valuable information on domain sizes can therefore be drawn from our ESR experiments. One can only estimate that the average domain sizes are larger than 6 nm. Combining ESR and NMR data, Bunge et al. [64] reported that the minimal radius of these nanodomains in POPC ternary mixture has to be in the order of 45–70 nm when approaching de-mixing temperature. Above the de-mixing temperature of 23.4 °C, for GUVs, the ESR data could identify as much as 70% of L_o fraction. It can be concluded that for POPC the observed homogeneous phase in GUVs is likely to be composed of a great number of L_o nano-scale domains invisible at the micron scale. In contrast, under the de-mixing temperature, a continuous L_o phase inside of which small L_d domains were distinguishable in GUVs.

4.5. Molecular interaction of POPC and PDPC with sphingomyelin and cholesterol

To further understand the molecular interactions between the neighboring lipid molecules with both PCs in the studied mixtures, data from low PC ternary (DSC) and binary PC/SM mixtures (ESR) were analyzed. A crucial point is related to the preferential interaction between SM and cholesterol that has been proposed as a key factor in the formation of cholesterol- and SM-rich domains in membranes [65]. Slotte and co-workers have shown the influence of the SM head group [66] or acyl-chain length [67], on L_o domain stabilization. The

ESR data indicate that a gel-liquid phase transition is observed for PDPC mixtures at a lower temperature compared to POPC, suggesting a higher miscibility of SM for PDPC. In contrast, the immiscibility observed in ternary mixtures containing cholesterol and PCs was shown to be due to the low affinity of cholesterol to polyunsaturated fatty acids [68].

Our DSC data could show PDPC lower miscibility in EggSM/chol/PC 85/10/5 mixtures compared to POPC. It suggests a higher PDPC affinity to SM rather than to cholesterol. The lower PDPC affinity to cholesterol was evidenced in the PDPC-containing mixtures, where a lower melting temperature for phase I and higher for phase II was observed. This later phase, proportionally more enriched with the cholesterol, exhibited a higher melting temperature and enthalpy (Table 2) indicating that more energy is required to melt this phase compared to the POPC-containing mixture. Our results support the idea that in the PDPC ternary mixtures, SM partition into L_o and L_d phases is rather governed by PDPC than cholesterol. The low affinity of cholesterol for PDPC in L_d phase can explain the observed cholesterol segregation into the L_o phase allowing more SM molecules to segregate along with cholesterol. The induced lipid packing leads to larger L_o domains in PDPC mixtures due to a reduction of the hydrophobic surface exposed to water molecules explaining the higher thermo-stability of this phase at physiological temperature and above. Interestingly, at lower temperatures the opposite trend is observed in ESR with increased L_o fraction for POPC mixture. Our data are in accordance with results reported by Stillwell and Wassall [69], using also OA and DHA, but in PE. Non-raft domains were also reported to exclude cholesterol because of the steric incompatibility between the highly disordered DHA acyl chain and the rigid steroid moiety of cholesterol [70] subsequently leading to an increased size of rafts [71]. The present ESR data are emphasizing the role of the temperature in the analysis of the results of detergent extraction in experiments comparing the PUFA content in DRM. The molecular order parameter and L_o fraction varies as a function of temperature with intersection of L_o domain fraction for POPC and PDPC at about 37 °C. Thus, the coefficient of partition of the detergent for the coexisting phases could be different at low (4 °C) and physiological temperature. The loosening effect of POPC in the L_o phase and smaller domain size can both allow more detergent to be partitioned and more cholesterol to be extracted.

The data shows that at low temperatures the greater the molar ratio of PCs in the ternary mixture, the larger the relative fraction of L_o domains. An explanation for this observation is that POPC and PDPC exhibit specific partition into the L_o domains, particularly at low temperatures (4 °C), the POPC seems to have more pronounced ability to partition into L_o compared to PDPC. Our results are in accordance with data coming from molecular simulations using hybrid lipids showing that POPC is able to partition into L_o domains, where such lipids decrease the order and compactness of the phase [72,73]. The authors also stated that the degree of unsaturation of the *sn-2* fatty acid chains characterizes the lineactant properties of the lipid with POPC being a weak lineactant compared to more unsaturated fatty acid lipids. The high propensity of POPC to form L_o nano domains in our studied mixtures could be the results of its modest ability to occupy lipid domain interface and reduce line tension.

4.6. Application for health and diseases

Very long-chain (n-3) fatty acids have been demonstrated to have a wide range of physiological roles that encompasses a beneficial effect on a number of risk factors for conditions such as cardiovascular disease [74]. There is also substantial evidence that these fatty acids are able to improve a number of key-pathways of the inflammation cascade among which the production of inflammatory cytokines and T cell reactivity [75]. Their physiological activities can positively impact conditions such as blood pressure regulation, thrombosis activity, and reduced inflammation. The anti-inflammatory aspects of PUFA have been tested via n-3 PUFA supplementation in several conditions such as e.g., arthritis, Crohn's disease, dermatitis, psoriasis, and ulcerative colitis processes [76]. Results of these supplementation studies need to be carefully examined as the animal model results do not compulsorily translate into human medicine [77,78]. Furthermore, an association with PUFA membrane modification and some medical conditions such as diabetes [79] or schizophrenia [80] has been described suggesting in some patients the existence of a throughout body membrane PUFA deficiency. Multiple molecular mechanisms involving (n-3) PUFA have been proposed. The connecting effects of PUFAs between the cell membranes, cytosol, and nucleus have been described modulating intracellular and extracellular signaling processes, and influencing patterns of gene expression as well as many other signaling pathways [81]. The here demonstrated changes in lateral lipid organization caused by PUFA composition have been proposed to account for the physiological effects of n-3 PUFAs, in particular in terms of membrane lipid order and protein sorting. An effect of PUFA in rafts was recently shown in several cell culture and animal studies influencing cell signaling in particular the activation T cell [82]. A modification in PUFA content in PC and PE may interfere differently in terms of signaling as PC is found primarily in the external leaflet where it is involved in rafts, while PE, internally located, being the major PUFA reservoir.

5. Conclusion

Using a combination of methods with both micron and submicron sensitivity, we have found in DHA vs OA containing PC mixtures that PDPC increases the Lo phase order parameter. In the studied mixtures, the lipid segregation does not only result from hydrophobic mismatch but also mode of acyl chain packing. A larger order parameter difference between L_o and L_d for PDPC is also involved in the phase separation. A comparison between GUV and ESR data indicates that above the demixing temperature POPC organizes in a great number of L_o nanoscale domains invisible at the micron scale, while under this temperature small L_d domains are distributed in a continuous L_o phase. The preferential affinity of PDPC to SM rather than to cholesterol is also to be considered, in particular as a function of temperature.

ESR data demonstrate that POPC and PDPC are able to partition into the liquid-ordered domains as POPC is more susceptible than PDPC. Overall, these result can shed some light on the role of the acid chain length and degree of unsaturation in the dynamic of raft-like domains in biological membranes where metastability is needed not only for a rapid response to biological stimuli but also to regulate physiological process such as inflammation and signaling.

Supplementary data to this article can be found online at http://dx.doi.org/10.1016/j.bbamem.2015.02.027.

Conflict of interest

The authors of the mentioned article declare that there are no conflicts of interest.

Acknowledgment

This work was supported by grants from the Bulgarian Fund for Scientific Research (DTK02/5/2009 and B02/23/2014). We thank Dr. Svetla Todinova for carrying out the DSC measurements. The authors are greatly indebted to Dr. Yves Frapart (UMR 8601, University René Descartes, 75005 Paris) for providing access to ELEXSYS 500 spectrometer Bruker.

References

[1] P.C. Calder, Marine omega-3 fatty acids and inflammatory processes: effects, mechanisms and clinical relevance, Biochim. Biophys. Acta 1851 (2015) 469–484.
[2] C.I. Janssen, A.J. Kiliaan, Long-chain polyunsaturated fatty acids (LCPUFA) from genesis to senescence: the influence of LCPUFA on neural development, aging, and neurodegeneration, Prog. Lipid Res. 53 (2014) 1–17.

[3] C.E. Ramsden, D. Zamora, B. Leelarthaepin, S.F. Majchrzak-Hong, K.R. Faurot, J.M. Davis, J.R. Hibbein, Use of dietary linoleic acid for secondary prevention of coronary heart disease and death: evaluation of recovered data from the Sydney diet heart study and updated meta-analysis, BMJ 346 (2013) e8707.
[4] H.F. Turk, R.S. Chapkin, Membrane lipid raft organization is uniquely modified by n-3 polyunsaturated fatty acids, Prostaglandins Leukot. Essent. Fatty Acids 88 (2013) 43–47.
[5] D. Lingwood, K. Simons, Lipid rafts as a membrane-organizing principle, Science 327 (2010) 46–50.
[6] D.A. Brown, E. London, Structure and origin of ordered lipid domains in biological membranes, J. Membr. Biol. 164 (1998) 103–114.
[7] C. Eggeling, C. Ringemann, R. Medda, G. Schwarzmann, K. Sandhoff, S. Polyakova, V.N. Belov, B. Hein, C. von Middendorff, A. Schonle, S.W. Hell, Direct observation of the nano-scale dynamics of membrane lipids in a living cell, Nature 457 (2009) 1159–1162.
[8] J.F. Hancock, Lipid rafts: contentious only from simplistic standpoints, Nat. Rev. Mol. Cell Biol. 7 (2006) 456–462.
[9] L.J. Pike, The challenge of lipid rafts, J. Lipid Res. 50 (2009) S323–S328.
[10] K. Jacobson, O.G. Mouritsen, R.G. Anderson, Lipid rafts: at a crossroad between cell biology and physics, Nat. Cell Biol. 9 (2007) 7–14.
[11] K. Simons, D. Toomre, Lipid rafts and signal transduction, Mol. Cell. Biol. 1 (2000) 31–41.
[12] B. Diaz-Rohrer, K.R. Levental, I. Levental, Rafting through traffic: membrane domains in cellular logistics, Biochim. Biophys. Acta 1838 (2014) 3003–3013.
[13] R. Koynova, M. Caffrey, Phases and phase transitions of the sphingolipids, Biochim. Biophys. Acta 1255 (1995) 213–236.
[14] C. Dietrich, L.A. Bagatolli, Z.N. Volovyk, N.L. Tompson, M. Levi, K. Jacobson, E. Gratton, Lipid rafts reconstituted in model membranes, Biophys. J. 80 (2001) 1417–1428.
[15] K. Bacia, P. Schwille, T. Kurzchalia, Sterol structure determines the separation of phases and the curvature of the liquid-ordered phase in model membranes, PNAS 102 (2005) 3272–3277.
[16] O. Bakht, P. Pathak, E. London, Effect of the structure of lipids favoring disordered domain formation on the stability of cholesterol-containing ordered domains (lipid rafts): identification of multiple raft-stabilization mechanisms, Biophys. J. 93 (2007) 4307–4318.
[17] R.F. de Almeida, A. Fedorov, M. Prieto, Sphingomyelin–phosphatidylcholine–cholesterol phase diagram: boundaries and composition of lipid rafts, Biophys. J. 85 (2003) 2406–2416.
[18] J. Zhao, J. Wu, H. Shao, F. Kong, N. Jain, G. Hunt, G. Feigenson, Phase studies of model biomembranes: macroscopic coexistence of La + Lb, with light-induced coexistence of La + Lo phases, Biochim. Biophys. Acta 1768 (2007) 2777–2786.
[19] E. London, How principles of domain formation in model membranes may explain ambiguities concerning lipid raft formation in cells, Biochim. Biophys. Acta 1746 (2005) 203–220.
[20] S.L. Veatch, S.L. Keller, Separation of liquid phases in giant vesicles of ternary mixtures of phospholipids and cholesterol, Biophys. J. 85 (2003) 3074–3083.
[21] S.M.K. Alanko, K.K. Halling, S. Maunula, J.P. Slotte, B. Ramstedt, Displacement of sterols from sterol/sphingomyelin domains in fluid bilayer membranes by competing molecules, Biochim. Biophys. Acta 1715 (2005) 111–121.
[22] R. Georgieva, K. Koumanov, A. Momchilova, C. Tessier, G. Staneva, Effect of sphingosine on domain morphology in giant vesicles, J. Colloid Interface Sci. 350 (2010) 502–510.
[23] O.B. Megha, E. London, Cholesterol precursors stabilize ordinary and ceramide-rich ordered lipid domains (lipid rafts) to different degrees: implications for the Bloch hypothesis and sterol biosynthesis disorders, J. Biol. Chem. 281 (2006) 21903–21913.
[24] G. Staneva, A. Momchilova, C. Wolf, P.J. Quinn, K. Koumanov, Membrane microdomains: role of ceramides in the maintenance of their structure and functions, Biochim. Biophys. Acta 1788 (2009) 666–675.
[25] G. Staneva, C. Chachaty, C. Wolf, K. Koumanov, P.J. Quinn, The role of sphingomyelin in regulating phase coexistence in complex lipid model membranes: competition between ceramide and cholesterol, Biochim. Biophys. Acta 1778 (2008) 2727–2739.
[26] W. Stillwell, S.R. Shaikh, M. Zerouga, R. Siddiqui, S.R. Wassall, Docosahexaenoic acid affects cell signaling by altering lipid rafts, Reprod. Nutr. Dev. 45 (2005) 559–579.
[27] A.G. Ayuyan, F.S. Cohen, Lipid peroxides promote large rafts: effects of excitation of probes in fluorescence microscopy and electrochemical reactions during vesicle formation, Biophys. J. 91 (2006) 2172–2183.
[28] S.E. Feller, K. Gawrisch, A.D. Mackernell, Polyunsaturated fatty acids in lipid bilayers: intrinsic and environmental contributions to their unique physical properties, J. Am. Chem. Soc. 124 (2001) 318–326.
[29] N.V. Eldho, S.E. Feller, S. Tristan-Nagle, I.V. Polozov, K. Gawrish, Polyunsaturated docosahexaenoic vs docosapentaenoic acid-differences in lipid matrix properties from the loss of one double bond, J. Am. Chem. Soc. 126 (2003) 6409–6421.
[30] L.L. Holte, S.A. Peter, T.M. Sinnwell, K. Gawrisch, 2H nuclear magnetic resonance order parameter profiles suggest a change of molecular shape for phosphatidycholines containing a polyunsaturated acyl chain, Biophys. J. 68 (1995) 2396–2403.
[31] D. Huster, J.J. Albert, K. Arnold, K. Gawrisch, Water permeability of polyunsaturated lipid membranes measured by ^{17}O NMR, Mol. Membr. Biol. 12 (1997) 131–134.
[32] J.M. Smaby, M.M. Momsen, H.L. Brockman, R.E. Brown, Phosphatidylcholine acyl unsaturation modulates the decrease in interfacial elasticity induced by cholesterol, Biophys. J. 73 (1997) 1492–1505.
[33] S.R. Shaikh, M.R. Brzustowicz, N. Gustafson, W. Stillwell, S.R. Wassall, Mono-unsaturated PE does not phase-separate from the lipid raft molecules sphingomyelin and cholesterol: role for polyunsaturation, Biochemistry 41 (2002) 10593–10602.
[34] N.F. Morales-Penningston, J. Wu, E.R. Farkas, S.L. Goh, T.M. Konyakhina, J.Y. Zheng, W.W. Webb, G.W. Feigenson, GUV preparation and imaging: minimizing artifacts, Biochim. Biophys. Acta 1798 (2010) 1324–1332.
[35] M. Angelova, D. Dimitrov, Liposome electroformation, Faraday Discuss. Chem. Soc. 81 (1986) 303–311.
[36] T.M. Konyakhina, S.L. Goh, J. Amazon, F.A. Heberle, J. Wu, G.W. Feigenson, Control of a nanoscopic-to-macroscopic transition: modulated phases in four-component DSPC/DOPC/POPC/Chol giant unilamellar vesicles, Biophys. J. 101 (2011) L08–L10.
[37] L.A. Bagatolli, E. Gratton, Direct observation of lipid domains in free-standing bilayers using two-photon excitation fluorescence microscopy, J. Fluoresc. 11 (2001) 141–160.
[38] A. Terzaghi, G. Tettamanti, M. Masserini, Interaction of glycoshingolipids in bilayers and plasma membranes of mammalian cells, Annu. Rev. Biophys. Chem. 14 (1993) 361–386.
[39] R.T. Zhang, R.M. Suter, J.F. Nagle, Theory of the structure factor of lipid bilayers, Phys. Rev. E 50 (1994) 5047–5060.
[40] T.J. McIntosh, The effect of cholesterol on the structure of phosphatidylcholine bilayers, Biochim. Biophys. Acta 513 (1978) 43–58.
[41] C. Chachaty, E.J. Soulié, Determination of electron spin resonance static and dynamic parameters by automated fitting of the spectra, J. Phys. III 5 (1995) 1927–1952.
[42] P. Jost, L.J. Libertini, V.C. Hebert, O.H. Griffith, Lipid spin labels in lecithin multilayers. A study of motion along fatty acid chains, J. Mol. Biol. 59 (1971) 77–98.
[43] B.J. Litman, E.N. Lewis, I.W. Levin, Packing characteristics of highly unsaturated bilayer lipids: Raman spectroscopic studies of multilamellar phosphatidylcholine dispersions, Biochemistry 30 (1991) 313–319.
[44] T.N. Estep, D.B. Mountcastle, R.L. Biltonen, T.E. Thompson, Studies on the anomalous thermotropic behaviour of aqueous dispersions of dipalmitoylpshosphatidylcholine–cholesterol mixtures, Biochemistry 17 (1978) 1984–1989.
[45] T.P.W. McMullen, R.N.A.H. Lewis, R.N. McElhaney, Differential scanning calorimetric study of the effect of cholesterol on the thermotropic phase behaviour of a homologous series of linear saturated phosphatidylcholines, Biochemistry 32 (1993) 516–522.
[46] T.P.W. McMullen, R.N. McElhaney, New aspects of the interactions of cholesterol with dipalmitoylphosphatidylcholine bilayers as revealed by high-sensitivity differential scanning calorimetry, Biochim. Biophys. Acta 1234 (1995) 90–98.
[47] T.P.W. McMullen, R.N. McElhaney, Physical studies of cholesterol–phospholipid interactions, Curr. Opin. Colloid Interface Sci. 1 (1996) 83–90.
[48] D.A. Mannock, T.J. McIntoch, X. Jiang, D.F. Covey, R.N. McElhaney, Effects of natural and enantiometric cholesterol on the thermotropic phase behaviour and structure of egg sphingomyelin bilayer membranes, Biophys. J. 84 (2003) 1038–1046.
[49] A. Radhakrishnan, H.M. Mc.Connell, Composition fluctuations, chemical exchange and nuclear relaxation in membranes containing cholesterol, J. Chem. Phys. 126 (2007) 185101–185107.
[50] K. Leidl, G. Liebisch, D. Richter, G. Schmitz, Mass spectrometric analysis of lipid species of human circulating blood cells, Biochim. Biophys. Acta 1781 (2008) 655–664.
[51] G. van Meer, D.R. Voelker, G.W. Feigenson, Membrane lipids: where they are and how they behave, Nature reviews Mol. Cell. Biol. 9 (2008) 112–124.
[52] D.R. Robinson, L.L. Xu, C.T. Knoell, S. Tateno, W. Olesiak, Modification of spleen phospholipid fatty acid composition by dietary fish oil and by n-3 fatty acid ethyl esters, J. Lipid Res. 34 (1993) 1423–1434.
[53] H.I. Ingolfsson, M.N. Melo, F.J. van Eerden, C. Arnarez, C.A. Lopez, T.A. Wassenaar, X. Periole, A.H. de Vries, D.P. Tieleman, S.J. Marrink, Lipid organization of the plasma membrane, J. Am. Chem. Soc. 136 (2014) 14554–14559.
[54] S.R. Shaikh, J.J. Kinnun, X. Leng, J.A. Williams, S.R. Wassall, How polyunsaturated fatty acids modify molecular organization in membranes: insight from NMR studies of model systems, Biochim. Biophys. Acta 1848 (2015) 211–219.
[55] H. Teague, R. Ross, M. Harris, D.C. Mitchell, S.R. Shaikh, DHA-fluorescent probe is sensitive to membrane order and reveals molecular adaptation of DHA in ordered lipid microdomains, J. Nutr. Biochem. 24 (2013) 188–195.
[56] H. Teague, C.J. Fhaner, M. Harris, D.M. Duriancik, G.E. Reid, S.R. Shaikh, n-3 PUFAs enhance the frequency of murine B-cell subsets and restore the impairment of antibody production to a T-independent antigen in obesity, J. Lipid Res. 54 (2013) 3130–3138.
[57] S.R. Shaikh, A.C. Dumaual, A. Castillo, D. LoCascio, R.A. Siddiqui, W. Stillwell, S.R. Wassall, Oleic and docosahexaenoic acid differentially phase separate from lipid raft molecules: a comparative NMR, DSC, AFM, and detergent extraction study, Biophys. J. 87 (2004) 1752–1766.
[58] J.A. Williams, S.E. Batten, M. Harris, B.D. Rockett, S.R. Shaikh, W. Stillwell, S.R. Wassall, Docosahexaenoic and eicosapentaenoic acids segregate differently between raft and nonraft domains, Biophys. J. 103 (2012) 228–237.
[59] H. Teague, M. Harris, J. Fenton, P. Lallemand, B.M. Shewchuk, S.R. Shaikh, Eicosapentaenoic and docosahexaenoic acid ethyl esters differentially enhance B-cell activity in murine obesity, J. Lipid Res. 55 (2014) 1420–1433.
[60] A.J. Garcia-Saez, S. Chiantia, P. Schwille, Effect of line tension on the lateral organization of lipid membranes, J. Biol. Chem. 282 (2007) 33537–33544.
[61] B.D. Rockett, H. Teague, M. Harris, M. Melton, J. Williams, S.R. Wassall, S.R. Shaikh, Fish oil increases raft size and membrane order of B cells accompanied by differential effects on function, J. Lipid Res. 53 (2012) 674–685.
[62] P.I. Kuzmin, S.A. Akimov, Y.A. Chizmadzhev, J. Zimmerberg, F.S. Cohen, Line tension and interaction energies of membrane rafts calculated from lipid splay and tilt, Biophys. J. 88 (2005) 1120–1133.
[63] C. Chachaty, D. Rainteau, C. Tessier, P.J. Quinn, C. Wolf, Building up of the liquid-ordered phase formed by sphingomyelin and cholesterol, Biophys. J. 88 (2005) 4032–4044.
[64] A. Bunge, P. Muller, M. Stockl, A. Hermann, D. Huster, Characterization of the ternary mixture of sphingomyelin, POPC, and cholesterol: support for inhomogeneous lipid distribution at high temperatures, Biophys. J. 94 (2008) 2680–2690.
[65] M. Lonnfors, J.P. Doux, J.A. Killian, T.K. Nyholm, J.P. Slotte, Sterols have higher affinity for sphingomyelin than for phosphatidylcholine bilayers even at equal acyl-chain order, Biophys. J. 100 (2011) 2633–2641.
[66] T.K. Nyholm, M. Nylund, J.P. Slotte, A calorimetric study of binary mixtures of dihydrosphingomyelin and sterols, sphingomyelin, or phosphatidylcholine, Biophys. J. 84 (2003) 3138–3146.

[67] B. Terova, R. Heczko, J.P. Slotte, On the importance of the phosphocholine methyl groups for sphingomyelin/cholesterol interactions in membranes: a study with ceramide phosphoethanolamine, Biophys. J. 88 (2005) 2661–2669.
[68] M.R. Brzustowicz, V. Cherezov, M. Caffrey, W. Stillwell, S.R. Wassall, Molecular organization of cholesterol in polyunsaturated membranes: microdomain formation, Biophys. J. 82 (2002) 285–298.
[69] R.S. Shaikh, A.C. Dumaual, D. Locassio, R.A. Siddiqui, W. Stillwell, Acyl chain unsaturation in PEs modulates phase separation from lipid raft molecules, Biochem. Biophys. Res. Commun. 311 (2003) 793–796.
[70] S.R. Shaikh, V. Cherezov, M. Caffrey, S.P. Soni, D. LoCascio, W. Stillwell, S.R. Wassall, Molecular organization of cholesterol in unsaturated phosphatidylethanolamines: X-ray diffraction and solid state ^{2}H NMR reveal differences with phosphatidylcholines, J. Am. Chem. Soc. 128 (2006) 5375–5383.
[71] S.P. Soni, D.S. LoCascio, Y. Liu, J.A. Williams, R. Bittman, W. Stillwell, S.R. Wassall, Docosahexaenoic acid enhances segregation of lipids between raft and non-raft domains: ^{2}H NMR study, Biophys. J. 95 (2008) 203–214.
[72] F.A. Heberle, M. Doktorova, S.L. Goh, R.F. Standaert, J. Katsaras, G.W. Feigenson, Hybrid and nonhybrid lipids exert common effects on membrane raft size and morphology, J. Am. Chem. Soc. 135 (2013) 14932–14935.
[73] E. Hassan-Zadeh, E. Baykal-Caglar, M. Alwarawrah, J. Huang, Complex roles of hybrid lipids in the composition, order and size of lipid membrane domains, Langmuir 30 (2014) 1361–1369.
[74] G. Michas, R. Micha, A. Zampelas, Dietary fats and cardiovascular disease: putting together the pieces of a complicated puzzle, Atherosclerosis 234 (2014) 320–328.
[75] P.C. Calder, n-3 fatty acids, inflammation and immunity: new mechanisms to explain old actions, Proc. Nutr. Soc. 72 (2013) 326–336.
[76] P.C. Calder, Mechanisms of action of (n-3) fatty acids, J. Nutr. 142 (2012) 592S–599S.
[77] P. Barberger-Gateau, C. Samieri, C. Feart, M. Plourde, Dietary omega 3 polyunsaturated fatty acids and Alzheimer's disease: interaction with apolipoprotein E genotype, Curr. Alzheimer Res. 8 (2011) 479–491.
[78] J.F. Quinn, R. Raman, R.G. Thomas, K. Yurko-Mauro, E.B. Nelson, C. Van Dyck, J.E. Galvin, J. Emond, C.R. Jack Jr., M. Weiner, L. Shinto, P.S. Aisen, Docosahexaenoic acid supplementation and cognitive decline in Alzheimer disease: a randomized trial, JAMA 304 (2010) 1903–1911.
[79] R.N. Weijers, Lipid composition of cell membranes and its relevance in type 2 diabetes mellitus, Curr. Diabetes Rev. 8 (2012) 390–400.
[80] P. Nuss, C. Tessier, F. Ferreri, M. De Hert, J. Peuskens, G. Trugnan, J. Masliah, C. Wolf, Abnormal transbilayer distribution of phospholipids in red blood cell membranes in schizophrenia, Psychiatry Res. 169 (2009) 91–96.
[81] J.A. Williams, S.E. Batten, M. Harris, B.D. Rockett, S.R. Shaikh, W. Stillwell, S.R. Wassall, Docosahexaenoic and eicosapentaenoic acids segregate differently between raft and nonraft domains, Biophys. J. 103 (2012) 228–237.
[82] W. Kim, Y.Y. Fan, R. Barhoumi, R. Smith, D.N. McMurray, R.S. Chapkin, n-3 Polyunsaturated fatty acids suppress the localisation and activation of signaling proteins at the immunological synapse in murine CD4+ T cells by affecting lipid raft formation, J. Immunol. 181 (2008) 6236–6243.